

Fair Latency-Aware Metric for real-time video segmentation networks

Evann Courdier^{1,2} Francois Fleuret¹

Abstract

As supervised semantic segmentation is reaching satisfying results, many recent papers focused on making segmentation network architectures faster, smaller and more efficient. In particular, studies often aim to reach the stage to which they can claim to be “real-time”. Achieving this goal is especially relevant in the context of real-time video operations for autonomous vehicles and robots, or medical imaging during surgery.

The common metric used for assessing these methods is so far the same as the ones used for image segmentation without time constraint: mean Intersection over Union (mIoU). In this paper, we argue that this metric is not relevant enough for real-time video as it does not take into account the processing time (latency) of the network. We propose a similar but more relevant metric called FLAME for video-segmentation networks, that compares the output segmentation of the network with the ground truth segmentation of the current video frame at the time when the network finishes the processing.

We perform experiments to compare a few networks using this metric and propose a simple addition to network training to enhance results according to that metric.

1. Introduction

Recent image segmentation networks are becoming good at producing visually accurate results and more and more focus is now given to designing architectures that are faster and can run on smaller hardware with less memory and computing power. In particular, enabling real-time segmentation is critical for applications in robotics, autonomous driving or medical imaging during surgery.

The main metric currently used to assess segmentation performance is the **mean Intersection over Union** (mIoU).

For networks aiming at speed, researchers also estimate efficiency with the **Frame Per Second** (FPS) metric, or its inverse the **Second Per Frame** metric also called **latency**.

To know if a given network will fit one’s needs, one usually separately assesses these two metrics, while they are intrinsically correlated. Moreover, a network claiming a good mIoU with a relatively long latency will usually produce a good segmentation of a scene that is no longer up-to-date. To the best of our knowledge, there are currently no metric that aims at assessing the usefulness of a network in a real-time setting. This confirms the relevance of a latency-aware metric capturing the real-time performance and “usefulness” of a network.

In the case of videos, we propose a novel Fair Latency-Aware MEtric (FLAME) that simply comes down to a different way of computing the mIoU, and is an attempt to combine both metrics by incorporating into the mIoU some information about the latency. We hope this metric can (1) help clarify what the objective of real-time networks should be and (2) represent a simple value practitioners can easily understand and check when searching for a network usable in real-time.

Our **contributions** are as follows:

- we propose a simple and relevant metric to assess real-time performance of video segmentation networks,
- we review what this metric depends on, and what new information it brings,
- we experimentally compare different networks with this metric and confirm its relevance,
- we consider different additions to the training process in order to optimize performance according to this metric.

We will make our code publicly available at the time of the conference if the paper is accepted.

2. Related Work

2.1. Image Semantic Segmentation

Most popular approaches for tackling Semantic Segmentation use a variant of powerful deep classification networks that have been made fully convolutional, with all final fully

¹Idiap Research Institute, Switzerland ²EPFL, Switzerland.
Correspondence to: Evann Courdier <evann.courdier@idiap.ch>.

connected layers replaced by convolutions. That idea is at the core of the FCN paper (Long et al., 2015).

The main issue coming with this technique is that it significantly reduces the image resolution to retrieve semantic information. Subsequent models for semantic segmentation are built on this “fully convolutional network” idea and attempt to cope with the dimension reductions, while increasing the Receptive Field.

One commonly used techniques is to use a **decoder network** plugged after the FCN to upsample the segmentation map using transposed convolution, as first did Ronneberger et al. (2015) and Badrinarayanan et al. (2017) with SegNet and U-Net. This setup allows to merge spatially rich shallow layers into semantically rich deeper layer.

Another successful technique is to avoid downsampling by using **dilated convolutions** (Yu et al., 2017) as was popularized for segmentation in DeepLab v2 (Chen et al., 2017). This allows to process a large field of view without having to reduce the image size, although it comes with the drawback of a larger computational complexity.

Finally, another successful idea is to add a so-called “**Spatial Pyramid Pooling**” module (He et al., 2015b) initially introduced for segmentation by Zhao et al. (2016). SPP pools the image simultaneously at different resolutions over a grid, which enlarges the Receptive Field. This allows to incorporate a larger context and to take into account higher-level semantic.

2.2. Real-time Semantic Segmentation

Reducing the computational cost and the memory cost of deep segmentation systems is critical for many applications that need to run real-time on slow hardware. One of the first to have been working toward this goal was ICNet (Zhao et al., 2017), which is a fast network that uses multi-scale processing with a special fuse block to merge those multi-scale information.

Among the different ways to design an efficient architecture, the first possibility is to use optimized blocks, for instance by factorizing kernels $k \times k$ into $1 \times k$ and $k \times 1$ kernels as is done by ERFNet (Romera et al., 2017), or by using group convolutions. In this case, there are different methods such as ShuffleNet (Zhang et al., 2018) to create connections between groups.

It is also possible to use depthwise separable convolution (DSC), which are the combination of depthwise and pointwise convolutions. These DSC are used to lower the number of parameters and makes the inference faster, at the cost of accuracy. They are used broadly in MobileNets (Howard et al., 2017; Sandler et al., 2018).

Another main idea from these network is to quickly down-

sample images in order to perform most of the processing at smaller resolution and never do full resolution processing. This idea is present in ENet (Paszke et al., 2016).

Finally, separating the localization problem from the semantic extraction problem and merging them appropriately as done in BiSeNet (Yu et al., 2018) is also a working technique.

A recent paper has used neural architecture search to discover neural architectures adapted to fast semantic segmentation, and in particular a network they named FasterSeg (Chen et al., 2019).

In this category, Swiftnet (Orsic et al., 2019) is another recent and relevant work. It is a lightweight Resnet followed by a simple decoder using lateral connections similarly to U-Net. It stands a bit aside insofar as its main strength and difference is actually to be pretrained on ImageNet. For our work, we choose SwiftNet as one of our base networks for its simplicity and its speed.

2.3. Video segmentation networks

Finally, another part of the literature focuses on designing **video** segmentation systems. More specifically, these works try to leverage the temporal correlation of consecutive frames in a video to improve the next-frame prediction and reduce computation and latency. However, most works in this domain are more focused on improving segmentation accuracy than reducing the latency.

The Clockwork net by Shelhamer et al. (2016) is a model that leverages temporal correlation by running different parts of the network at each time-step conditionally to how much the video has changed from the previous frame. This technique has the disadvantage of not providing a fixed frame-rate.

Another direction to address the problem is to try propagating previous features to consecutive frames to avoid recomputing very similar features for following frames, as do Zhu et al. (2016), though their design still keeps it too slow for real-time.

Li et al. (2018) built on these two previous ideas. Their network decides at each frame whether to propagate previous features or to recompute the entire segmentation map. They improved the clockwork design to reduce the maximum latency but did not reach real-time.

Other works use predictive learning, that is predicting future frames or flow motion using past frames and segmentations to help current segmentation (Jin et al., 2017a;b).

Gadde et al. (2017) are using video temporal coherence to produce better output segmentation maps through representation warping, and are not focused on time efficiency.

Finally, a recent paper by Zhang et al. (2019) is proposing a fast segmentation network using a Dynamic Targeting Network and a Mask Refinement Network that respectively locates the segmentation target and predicts the segmentation.

3. A latency-aware metric

3.1. The mean Intersection over Union

The Intersection over Union metric is surely one of, if not the most commonly used method to assess the correctness of a segmentation mask. It is by definition stronger than both precision and recall, which makes it a good candidate for strong metric. It is defined as follow:

$$\text{IoU} = \frac{TP}{TP + FP + FN} = \frac{|GT \cap Pred|}{|GT \cup Pred|} \quad (1)$$

With TP : True Positive, FP : False Positive, FN : False Negative, GT : Ground Truth.

The last equality is where the metric takes its name: we divide the intersection of the ground truth and the predicted areas by the union of these same areas.

As there usually are a few dozens a classes on a image, we take the mean of all the IoU of each class to get the mean IoU: mIoU.

Finally, note that in the case of the mIoU of multiple images, one do not average again single mIoUs to get another value. Rather, for a given class, we consider every image when computing the union and intersection. The formula for K classes and N images is then:

$$mIoU = \frac{1}{K} \sum_{k=1}^K \frac{\sum_{i=1}^N |GT_{i,k} \cap Pred_{i,k}|}{\sum_{i=1}^N |GT_{i,k} \cup Pred_{i,k}|} \quad (2)$$

3.2. A latency-aware mean Intersection over Union

In order to give more meaning to the mIoU value when it is used for real-time video applications, we propose to make it "latency aware". The "latency-aware" mIoU, named FLAME, is the mIoU between the segmentation mask in output of the network and the ground truth segmentation of the current image **at the time the network finishes its computation**.

Let us consider a video sequence and let I_t and S_t denote respectively the frame at time t and its ground truth segmentation. Let F denote the operation of a semantic segmentation network that processes one image in l_F milliseconds. The common way to assess performance is to compute:

$$mIoU(F(I_t), S_t) \quad (3)$$

while our metric proposes to consider:

$$mIoU(F(I_t), S_{t+l_F}) \quad (4)$$

The only change is the addition of l_F . Instead of predicting the segmentation of the current frame, our FLAME metric expects systems to predict the segmentation of a future frame, thus acknowledging the prediction time.

We claim this metric is particularly relevant for real-time applications in which we are usually interested in what is currently happening, and not what was a few instant back. It is indeed relevant to compare the information we get at a given time using a network ($F(I_t)$) with the information we ideally would like to get at that time (S_{t+l_F}).

In practice, a video sequence does not have a continuous set of frames. In this case, we pick the frame **appearing next** after the model has output a segmentation.

More precisely, let's assume without loss of generality that $t = 0$ when frame of index 0 enters the network and consider a video sequence with a delay d between two frames ($\text{fps} = 1/d$). Then, the index of the segmentation that the metric would use as ground truth is:

$$k_F = \lceil l_F/d \rceil \quad (5)$$

In the following, when we refer to $t + k_F \times d$, we will abuse notation and write $t + k_F$.

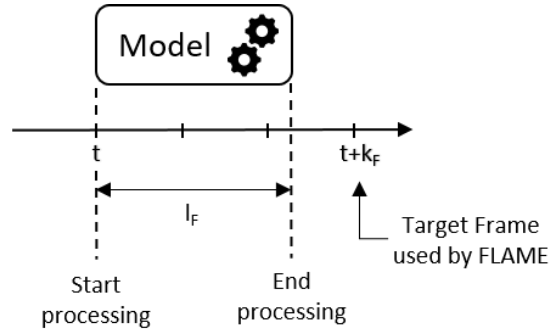


Figure 2. Definition of the frame used in the FLAME metric

3.3. Information brought by the metric

This new FLAME metric indicates the match of the current scene with what our network outputs at that time. The longer the network takes in processing, the less accurate it will be at predicting the segmentation of the frame coming after that processing.

More importantly, **the metric gives directly an insight of how good and useful a network is in a real-time setting**, without having to juggle with the static mIoU and the FPS.

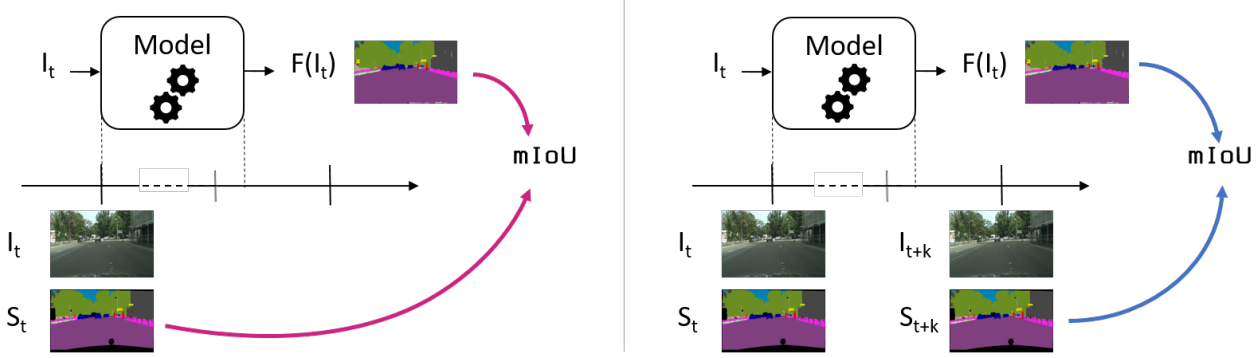


Figure 1. Left: How mIoU is computed now ; the output of the network is compared to the ground truth segmentation of the *image in input of the network*. Right: Our proposed way to measure mIoU ; the output of the network is compared to the ground truth segmentation of the *current image* when network finishes processing.

It does not give information about whether the network is actually fast enough to work in real-time, but rather about how good it would be if we suppose it is. Note that a network does not need to be "real-time" strictly speaking for the metric to make sense. For a network reaching a few frames per second, the metric would still provide useful information.

This metric also brings to light the fact that a real-time video segmentation network should be trained to predict a future segmentation, and in particular the segmentation of the frame which will be current when it finishes the processing. Additionally, these networks should be ranked according to how well they anticipate the future and take into account their own latency.

3.4. What the metric depends on

Due to its latency-aware property, the FLAME metric is also more sensitive to the setting in which it is computed than a usual metric.

The **hardware** - what kind of GPU device is it running on - has a great influence on the latency. Therefore, it also has a similar influence on our metric. A given network will have a different value of the latency-aware metric per hardware. This is actually a good feature as it can help choose the right hardware depending on one's precision need.

The **dataset**, and notably its **sampling frequency**, has a strong impact on the metric. In particular, the higher the frame-rate of the video dataset, the more precise and useful the metric will be. Indeed, if the time between two frames is too long, it won't allow fine grained difference between networks whose latency are close. In the worst case, the time between two frames is bigger than the two networks

processing times, in which case this metric will be less informative.

We see here the importance of having a good quality dataset with high sampling frequency for the latency-aware metric to provide us with useful measurements.

4. Dataset and experimental setup

4.1. Dataset

As video sequence dataset, we chose the CityScapes¹ dataset (Cordts et al., 2016) to conduct our experiments. This dataset contains 2,975 training, 500 validation and 1,525 testing video sequences. Each sequence contains 30 frames, the 20th of which is annotated with fine pixel-level class labels for 19 object categories. A sequence is 1.8s long, which gives a framerate of approximately 16.6 fps and there are around 60ms between each frame.

We chose Cityscapes for the presence of video sequences and its widespread use as a segmentation benchmark. However, Cityscapes sequences have a little low framerate, which means the time between two images is a little long, which reduces the accuracy of our metric.

As Cityscapes contains only the ground truth segmentation for one image per sequence, we have to process as follows:

1. We time the latency l_F of the network
2. We determine how many frames of offset k_F this time corresponds to: $k_F = \lceil l_F / 0.06 \rceil$ ($0.06 = 60\text{ms}$)
3. We use as input of the network the frame of index $20 - k_F$ since we always have only the 20th frame's

¹<https://www.cityscapes-dataset.com/>

ground truth segmentation

4.2. Networks

For our experiments, we chose 2 network architectures. We picked SwiftNet (Orsic et al., 2019) and DeepLab-V3+ (Chen et al., 2018) with 2 different encoders : Resnet-101 and MobileNet v2 (Sandler et al., 2018).

4.2.1. SWIFNET

SwiftNet is a state of the art network in real-time segmentation. For our experiments, we have built this network as it is described in the original paper. For convenience, we briefly describe it below. It is a network with an encoder-decoder structure:

- The encoder backbone is a classical Resnet-18 whose fully connected layers have been removed to make it fully convolutional.
- A Spatial Pyramid Pooling Module with 4 different pooling layers of grid size (1,2,4,8) is plugged in output of the encoder to increase its receptive field.
- Finally, a decoder with 3 upsampling modules recovers original image resolution. An upsampling module upsamples the previous layer’s output and then merges it with a skip connection coming from the encoder.

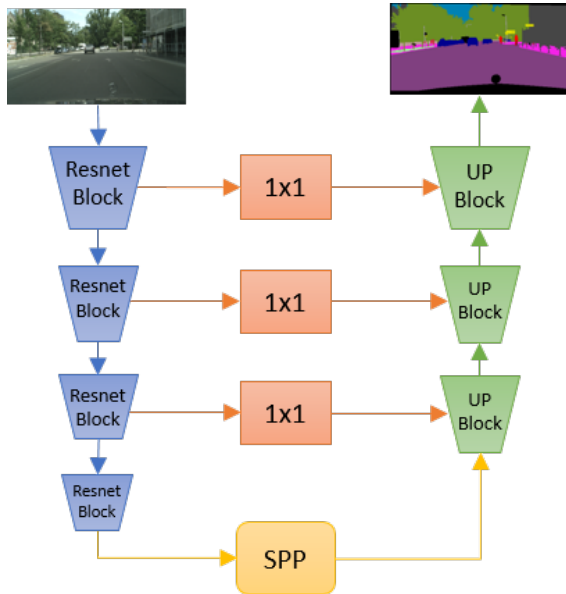


Figure 3. SwiftNet architecture

We will refer to it as **SwiftNet-R18**. It has approximately 12M parameters. On Cityscapes, it reaches 75% mIoU and runs at about 40 fps on a GTX 1080 Ti. On this hardware,

SwiftNet has a latency of 26 ms. This means we have to use $k_F = 1$ frame offset to compute the FLAME performance.

We will also consider a variant of this network, since we noticed experimentally that expending the number of channels after the initial convolution helped reach higher performance.

More specifically, we replace the first layer of the original SwiftNet:

$$\text{conv}(3, 64, 7 \times 7, s = 2)$$

with the following block of four layers:

$$\text{conv}(3, 130, 7 \times 7, s = 2)$$

$$\text{BN}(130)$$

$$\text{ReLU}$$

$$\text{conv}(130, 64, 3 \times 3, s = 1).$$

The newly created convolutions were initialized using He’s initialization (He et al., 2015a). We will refer to our updated SwiftNet version as **SwiftNet-R18-X** for eXtended.

4.2.2. DEEPLAB V3+

DeepLab v3+ is a state of the art network in image segmentation. We have followed original paper instructions for the code of these networks. We will briefly describe it below as well. It has an encoder-decoder architecture very similar to that of SwiftNet:

- We used two different encoder backbones :
 - One backbone is a dilated Resnet-101 network stripped of its fully connected layers. We use an output stride of 16, so the last two Resnet blocks are using dilated convolutions to enlarge the receptive field.
 - The other backbone is a MobileNet-V2 network as described by Sandler et al. (2018). It uses depthwise separable convolutions inside “inverted” residuals blocks separated by linear bottlenecks.
- An Atrous Spatial Pyramid Pooling module is plugged after this encoder. It convolves the encoder output with 4 atrous convolutions using different dilation rates: (1, 6, 12, 18).
- Finally, a small decoder upsamples the ASPP output and concatenates it with low-level features from the encoder. The decoder blends them with a convolution and upsamples the output to the original image size.

When using a Resnet-101 as backbone, the whole network has approximately 60M parameters and reaches 77% mIoU on Cityscapes but runs at 5 fps only. We will refer to it as

Table 1. Results of the 3 experiments for each of the 4 networks. The first line gives the static mIoU, the next three lines reports value of the FLAME metric for different training configurations. The last three lines gives information about latency, frame offset used for the network as explained in 4.1, and fps of these networks. Note that the k temporal offset depends on the network, hardware and dataset framerate, and is greater and leads to poorer performance for slow processing.

	Input	Target (train)	Target (test)	DeepLab-R101	DeepLab-MN	SwiftNet-R18	SwiftNet-R18-X
FLAME	I_t	S_t	S_t	0.77	0.72	0.75	0.735
	I_t	S_t	S_{t+k}	0.495	0.56	0.64	0.63
	I_t	S_{t+k}	S_{t+k}	0.53	0.565	0.65	0.635
	I_{t-1}, I_t	S_{t+k}	S_{t+k}	0.60	0.58	0.67	0.685
Frame offset (k)				4	2	1	1
Latency (ms)				195	76	26	38
FPS				5	13	38	26

DeepLab-R101. On our hardware, it has a latency of 195 ms, which means we have to use $k_F = 4$ frame offsets to compute the FLAME performance.

When using a MobileNet backbone, the model has about 5.5M parameters. It reaches 72% mIoU on Cityscapes and runs at 13 fps. We will refer to it as **DeepLab-MN**. It has a latency of 76 ms, so we have to use $k_F = 2$ frame offsets to compute the FLAME performance.

4.3. Training

We coded our experiments using the PyTorch framework. All encoders in our network were pretrained on the ImageNet-1k dataset. We used pretrained network weights provided in the library.

Data augmentation We used image crops of 768×768 . We did standard image augmentation with random horizontal flip, random scaling from 0.75 to 1.5 and random gaussian blur.

SwiftNet For SwiftNet, we used a batch size of 12 and trained using Adam optimiser with default parameters. We used a learning rate of $5e^{-4}$ and a weight decay of $1e^{-4}$. We also set a smaller learning rate of $1e^{-4}$ for the part that was ImageNet-pretrained. We trained the network for 200 epochs and used a cosine annealing schedule with $\eta_{min} = 1e^{-6}$.

DeepLab v3+ For DeepLab, we used a batch size of 10 and trained using SGD optimiser with momentum of 0.9. We used a learning rate of $5e^{-2}$ and a weight decay of $5e^{-4}$. We similarly set a smaller learning rate of $5e^{-3}$ for the part that was ImageNet-pretrained. We trained the network for 220 epochs and used a poly schedule with a power of 3.

Hardware We train all networks on a Tesla P40 GPU device. We run all our timing experiments on a GTX 1080 Ti GPU device.

5. Experiments and Experimental Results

We perform 3 different successive experiments. For each experiments, the only parameters that changes are the inputs and targets used for training and testing.

5.1. First experiment

In the first experiment, we simply evaluates the 4 networks with the FLAME metric previously defined. The networks are trained “as usual”: input is I_t and target is S_t .

The results are reported in second line of table 1. Compared to their usual mIoU, we can notice a significant drop from 10% to 30 %.

5.2. Second experiment

In the second experiment, the networks are trained to predict the segmentation ground-truth that our FLAME metric is using: we use as input I_t and as target S_{t+k} . Here k is different for each network as each has a different latency and will therefore be tested against a different segmentation ground-truth.

The results are reported in third line of table 1. We can see a slight but consistent increase of the metric for all networks. We reported on figure 4 examples of the output segmentation of SwiftNet-R18 overlaid on image I_t and I_{t+1} .

We can notice the segmentation mask is slightly blurry, as could be expected. However, in multiple cases, we can note the interesting fact that the blur is anisotropic, meaning it is not a blur all around the object, but rather promoting a specific direction.

It turns out the network is able to predict some objects movement based on their orientation. For instance, people facing left in I_t are likely to have moved left in the next image I_{t+1} . Similarly, if it detects the front of a car, it can infer that the car is coming toward the camera and thus is

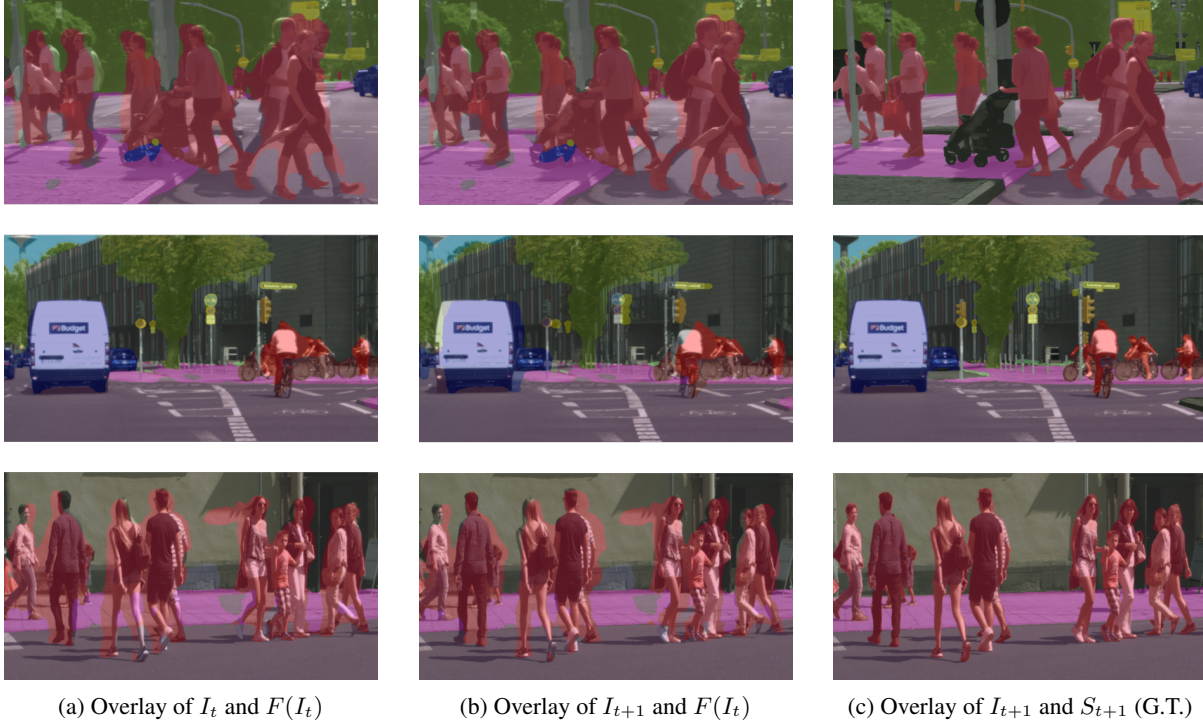


Figure 4. Output segmentation of SwiftNet-R18 trained to predict S_{t+1} from I_t . We observe anisotropic blur as the network is able to infer some objects probable movement directions from their orientation.

likely to look bigger in the next frame.

However, the network has no way to infer the relative speed of different instances in the images which makes its prediction relatively inaccurate.

5.3. Third experiment

In the third experiment, the networks are still trained to predict the FLAME segmentation ground-truth S_{t+k} , but now we use as input both I_{t-1} and I_t .

The results are reported in fourth line of table 1. We can see a consistent improvement of the metric. It is clear that using an additional input in the network is useful here for producing sharper and more accurate segmentation maps.

Here, thanks to the two images in input, the network has a way of determining directions and relative instant speed of the different elements in the image. Therefore, it is able to predict a much more accurate segmentation of the next frame. We reported on figure 5 examples of the output segmentation of SwiftNet-R18 overlaid on image I_t and I_{t+1} .

5.4. Additional experiment

We had the intuition that it is important for the network to have a big Receptive Field when processing simultaneously images from different time-steps I_{t-1} and I_t . In order to

obtain a bigger field of view without having to use big filters, we tried to offset part of this work on the input.

The idea is to concatenate to the current inputs of the SwiftNet network various translations of the previous image I_{t-1} . Particularly, we changed the inputs $\{I_{t-1}, I_t\}$ of the previous experiment to $\{T_1(I_{t-1}), \dots, T_N(I_{t-1}), I_{t-1}, I_t\}$. corresponding to N different fixed translations T_i .

The translations offsets were chosen to span a regular grid around the origin. We experimented with different numbers of translations in input: $N = 9$, $N = 17$, $N = 25$ and $N = 81$.

The intuition behind the use of translations is to trade part of the computational cost usually associated with the use of big convolutional kernels for the memory cost of having more inputs. Using translations would compensate the use of big kernels by allowing the model to simultaneously attend different parts of the image that would normally be processed separately by a normal convolution kernel.

While initial experiments seemed promising, we discovered that setting all translation offsets to zero yielded nearly identical results. Setting all translation offsets to zero amounts to using as inputs of the network multiple copies of I_{t-1} .

In this setting, the only structural difference remaining with the original SwiftNet model is an additional convolutional layer added at the input of the model to account for the translations. More explicitly, in the case of N translations,



Figure 5. Output segmentation of SwiftNet-R18 trained to predict S_{t+1} from (I_{t-1}, I_t) . We observe a more precise segmentation as the network has a way to infer relative speeds and directions.

we had replaced:

$$\text{conv}(3, 64, 7 \times 7, s = 2)$$

with the following block:

$$\begin{aligned} &\text{conv}(6 + 3 \times N, 8 \times N, 7 \times 7, s = 2) \\ &\text{BN}(8 \times N) \\ &\text{ReLU} \\ &\text{conv}(8 \times N, 64, 3 \times 3, s = 1). \end{aligned}$$

The number of output channels of the first convolution is dependant on the number of translations used. We notice that the best results were obtained with 17 translations and deduced that the main reason for these results was the increase of the number of channels in output of the first convolution. This remark eventually lead to the design of SwiftNet-R18-X described in section 4.2, which is indeed slightly more performant according to the FLAME metric when using I_{t-1} and I_t as inputs.

6. Conclusion

In this paper, we have introduced a new simple metric for real-time semantic segmentation. Our proposed metric sums up in one value information about how successful a network is in such a setting by assessing how the prediction matches the ground truth, taking into account not only the computation speed, but the resulting latency. More generally, we

introduced a different way of computing any existing metric and to make it meaningful for real-time video processing.

In proposing such a metric, we have also emphasized that, due to non-instantaneous computation, a real-time network actually has to make a prediction which is in the future of the available input.

Finally, through our experiments we have seen that a real-time segmentation network should make use of a few of the previous images to be able to estimate speed and directions of elements in a scene, and infer future positions of objects. We have also shown that increasing the number of channels early in the processing of the SwiftNet network allows to improve performance in that context.

References

- Badrinarayanan, V., Kendall, A., and Cipolla, R. Segnet: A deep convolutional encoder-decoder architecture for image segmentation. *IEEE transactions on pattern analysis and machine intelligence*, 39(12):2481–2495, 2017.
- Chen, L.-C., Papandreou, G., Kokkinos, I., Murphy, K., and Yuille, A. L. Deeplab: Semantic image segmentation with deep convolutional nets, atrous convolution, and fully connected crfs. *IEEE transactions on pattern analysis and machine intelligence*, 40(4):834–848, 2017.
- Chen, L.-C., Zhu, Y., Papandreou, G., Schroff, F., and Adam, H. Encoder-Decoder with Atrous Sep-

- arable Convolution for Semantic Image Segmentation (DeepLabv3+). *arXiv:1802.02611 [cs]*, February 2018. URL <http://arxiv.org/abs/1802.02611>. arXiv: 1802.02611.
- Chen, W., Gong, X., Liu, X., Zhang, Q., Li, Y., and Wang, Z. Fasterseg: Searching for faster real-time semantic segmentation. *arXiv preprint arXiv:1912.10917*, 2019.
- Cordts, M., Omran, M., Ramos, S., Rehfeld, T., Enzweiler, M., Benenson, R., Franke, U., Roth, S., and Schiele, B. The cityscapes dataset for semantic urban scene understanding. In *Proceedings of the IEEE conference on computer vision and pattern recognition*, pp. 3213–3223, 2016.
- Gadde, R., Jampani, V., and Gehler, P. V. Semantic Video CNNs through Representation Warping. *arXiv:1708.03088 [cs]*, August 2017. URL <http://arxiv.org/abs/1708.03088>. arXiv: 1708.03088.
- He, K., Zhang, X., Ren, S., and Sun, J. Delving deep into rectifiers: Surpassing human-level performance on imagenet classification. In *Proceedings of the IEEE international conference on computer vision*, pp. 1026–1034, 2015a.
- He, K., Zhang, X., Ren, S., and Sun, J. Spatial pyramid pooling in deep convolutional networks for visual recognition. *IEEE transactions on pattern analysis and machine intelligence*, 37(9):1904–1916, 2015b.
- Howard, A. G., Zhu, M., Chen, B., Kalenichenko, D., Wang, W., Weyand, T., Andreetto, M., and Adam, H. MobileNets: Efficient Convolutional Neural Networks for Mobile Vision Applications. *arXiv:1704.04861 [cs]*, April 2017. URL <http://arxiv.org/abs/1704.04861>. arXiv: 1704.04861.
- Jin, X., Li, X., Xiao, H., Shen, X., Lin, Z., Yang, J., Chen, Y., Dong, J., Liu, L., Jie, Z., et al. Video scene parsing with predictive feature learning. In *Proceedings of the IEEE International Conference on Computer Vision*, pp. 5580–5588, 2017a.
- Jin, X., Xiao, H., Shen, X., Yang, J., Lin, Z., Chen, Y., Jie, Z., Feng, J., and Yan, S. Predicting scene parsing and motion dynamics in the future. In *Advances in Neural Information Processing Systems*, pp. 6915–6924, 2017b.
- Li, Y., Shi, J., and Lin, D. Low-latency video semantic segmentation. In *Proceedings of the IEEE Conference on Computer Vision and Pattern Recognition*, pp. 5997–6005, 2018.
- Long, J., Shelhamer, E., and Darrell, T. Fully convolutional networks for semantic segmentation. In *Proceedings of the IEEE conference on computer vision and pattern recognition*, pp. 3431–3440, 2015.
- Orsic, M., Kreso, I., Bevandic, P., and Segvic, S. In defense of pre-trained imagenet architectures for real-time semantic segmentation of road-driving images. In *Proceedings of the IEEE conference on computer vision and pattern recognition*, pp. 12607–12616, 2019.
- Paszke, A., Chaurasia, A., Kim, S., and Culurciello, E. Enet: A deep neural network architecture for real-time semantic segmentation. *arXiv preprint arXiv:1606.02147*, 2016.
- Romera, E., Alvarez, J. M., Bergasa, L. M., and Arroyo, R. Erfnet: Efficient residual factorized convnet for real-time semantic segmentation. *IEEE Transactions on Intelligent Transportation Systems*, 19(1):263–272, 2017.
- Ronneberger, O., Fischer, P., and Brox, T. U-net: Convolutional networks for biomedical image segmentation. In *International Conference on Medical image computing and computer-assisted intervention*, pp. 234–241. Springer, 2015.
- Sandler, M., Howard, A., Zhu, M., Zhmoginov, A., and Chen, L.-C. Mobilenetv2: Inverted residuals and linear bottlenecks. In *Proceedings of the IEEE conference on computer vision and pattern recognition*, pp. 4510–4520, 2018.
- Shelhamer, E., Rakelly, K., Hoffman, J., and Darrell, T. Clockwork Convnets for Video Semantic Segmentation. *arXiv:1608.03609 [cs]*, August 2016. URL <http://arxiv.org/abs/1608.03609>. arXiv: 1608.03609.
- Yu, C., Wang, J., Peng, C., Gao, C., Yu, G., and Sang, N. BiSeNet: Bilateral Segmentation Network for Real-time Semantic Segmentation. *arXiv:1808.00897 [cs]*, August 2018. URL <http://arxiv.org/abs/1808.00897>. arXiv: 1808.00897.
- Yu, F., Koltun, V., and Funkhouser, T. Dilated residual networks. In *Proceedings of the IEEE conference on computer vision and pattern recognition*, pp. 472–480, 2017.
- Zhang, L., Lin, Z., Zhang, J., Lu, H., and He, Y. Fast video object segmentation via dynamic targeting network. In *Proceedings of the IEEE International Conference on Computer Vision*, pp. 5582–5591, 2019.
- Zhang, X., Zhou, X., Lin, M., and Sun, J. Shufflenet: An extremely efficient convolutional neural network for mobile devices. In *Proceedings of the IEEE conference on computer vision and pattern recognition*, pp. 6848–6856, 2018.

Zhao, H., Shi, J., Qi, X., Wang, X., and Jia, J. Pyramid Scene Parsing Network (PSPNet). *arXiv:1612.01105 [cs]*, December 2016. URL <http://arxiv.org/abs/1612.01105>. arXiv: 1612.01105.

Zhao, H., Qi, X., Shen, X., Shi, J., and Jia, J. ICNet for Real-Time Semantic Segmentation on High-Resolution Images. *arXiv:1704.08545 [cs]*, April 2017. URL <http://arxiv.org/abs/1704.08545>. arXiv: 1704.08545.

Zhu, X., Xiong, Y., Dai, J., Yuan, L., and Wei, Y. Deep Feature Flow for Video Recognition. *arXiv:1611.07715 [cs]*, November 2016. URL <http://arxiv.org/abs/1611.07715>. arXiv: 1611.07715.